States of seniority 3 and 5 in the $N=48$ nucleus ^{87}Y

R. Schwengner, J. Reif,* H. Schnare, G. Winter,† T. Servene, L. Käubler, and H. Prade
Institut für Kern- und Hadronenphysik, Forschungszentrum Rossendorf, D-01314 Dresden, Germany

M. Wilhelm, A. Fitzler, S. Kasemann, E. Radermacher, and P. von Brentano
Institut für Kernphysik, Universität zu Köln, D-50937 Köln, Germany

(Received 30 January 1998)

Excited states of the nucleus ^{87}Y were investigated via the reaction ^{80}Se(^{11}B,$4n$) at 45 MeV. γ rays were detected with the six-detector array OSIRIS CUBE. The level scheme of ^{87}Y has been extended up to $J^\pi = 33/2^{(-)}$ at $E \approx 7$ MeV. Mean lifetimes of eight levels have been deduced using the Doppler-shift-attenuation method. The structure of ^{87}Y has been interpreted in terms of the shell model. The calculations performed in the model space $\pi(0f_{5/2},1p_{3/2},1p_{1/2},0g_{9/2})\nu(1p_{1/2},0g_{9/2})$ well reproduce experimental excitation energies and transition strengths in ^{87}Y, especially the large $B(M1)$ values of up to 1.8 W.u. between yrast states with $J > 21/2$. Structural differences between ^{87}Y and the isotone ^{85}Rb are discussed on the basis of the shell-model calculations. [S0556-2813(98)01306-5]

PACS number(s): 21.10.Tg, 21.60.Cs, 23.20.−g, 27.50.+e

I. INTRODUCTION

In our investigation of the $N=48$ nuclei ^{83}Br ($Z=35$) and ^{85}Rb ($Z=37$) a variety of structural phenomena has been observed [1,2]. The yrast sequences of these nuclei display regular level spacings and weakly collective $E2$ transition strengths of $B(E2) \approx 15$ Weisskopf units (W.u.) up to $J^\pi = 17/2^+$. At higher spin positive-parity as well as negative-parity states form multipletlike $\Delta J = 1$ sequences including strong $M1$ transition strengths of up to $B(M1) \approx 1$ W.u. In shell-model calculations using the model space $\pi(0f_{5/2},1p_{3/2},1p_{1/2},0g_{9/2})\nu(0g_{9/2},1p_{1/2})$ the weakly collective properties of the $9/2^+, 13/2^+, 17/2^+$ states result from a coherent superposition of many contributing components including $\pi(fp)$ and $\nu 0g_{9/2}^{-2}$ excitations. The positive-parity states with $21/2^+ \leqslant J^\pi \leqslant 33/2^+$ are described as members of seniority $v=3$ and $v=5$ multiplets arising from a recoupling of the spins of the involved $\pi(0f_{5/2}^{-1}1p_{3/2}^{-1}0g_{9/2}^{1})$ and $\nu(0g_{9/2}^{-2})_8$ orbitals. This recoupling generates the large $B(M1)$ values [3].

To extend the knowledge of the nuclear structure at $N=48$ to nuclei with larger proton numbers we have studied the nucleus ^{87}Y ($Z=39$). Excited states in this nucleus were previously studied in the ^{89}Y(p,t) transfer reaction [4] and via ^{85}Rb(α,$2n$) [5] and ^{74}Ge(^{18}O,$p4n$) [6] reactions. In those studies excited states up to $E \approx 4.6$ MeV were observed.

In the present work the level scheme of ^{87}Y has been extended up to $J^\pi = 33/2^{(-)}$ at $E \approx 7$ MeV. Several level placements and spin-parity assignments have been altered with respect to previous work. Mean lifetimes of eight levels have been determined using the Doppler-shift-attenuation (DSA) method.

II. EXPERIMENTAL METHODS AND RESULTS

Excited states in ^{87}Y were populated via the reaction ^{80}Se(^{11}B,$4n$) at $E=45$ MeV using the ^{11}B beam of the FN tandem accelerator of the University of Cologne. The target consisted of a 2.3 mg cm^{-2} thick layer of ^{80}Se enriched to 99.1% on a gold backing of thickness 2.5 mg cm^{-2}. γ rays were detected with the six-detector array OSIRIS CUBE [7]. Singles spectra were recorded in parallel with γ-γ coincidences with the Cologne FERA analyzer [8]. A total of 3×10^8 γ-γ coincidences was measured and sorted off-line into $E_\gamma - E_\gamma$ matrices for either all or selected detector combinations. Coincidence spectra were extracted by setting gates on certain peak and background intervals in the E_γ–E_γ matrices using the codes ESCL8R [9] and VS [10]. Examples of background-corrected coincidence spectra are shown in Fig. 1. The γ rays assigned to ^{87}Y on the basis of the present coincidence experiment are compiled in Table I.

A. Gamma-gamma directional correlations

In connection with the coincidence experiment the analysis of directional correlations of coincident γ rays emitted from oriented states (DCO) was applied to deduce the multipole order of the γ rays and thus to derive multipole mixing ratios and to assign spins to the emitting states. This method is based on the formalism described in Refs. [11,12] and discussed, e.g., in Ref. [13]. The DCO ratio is defined as $R_{\rm DCO} = W(\theta_1,\theta_2,\phi)/W(\theta_2,\theta_1,\phi)$, where the quantity $W(\theta_1,\theta_2,\phi)$ denotes the coincidence intensity of a transition γ_2 measured in a detector at the angle θ_2 relative to the beam, gated with a transition γ_1 measured in a detector at the angle θ_1. The quantity ϕ is the angle between the two planes opened by the respective target-detector axis and the beam axis. The intensity $W(\theta_2,\theta_1,\phi)$ describes the reverse case arising from an exchange of the observation angles or of the gating and observed transition. A ratio of $R_{\rm DCO}=1$ is obtained if the transitions γ_1 and γ_2 are stretched transitions of pure and equal multipole order.

*Present address: Heyde+Partner, 01099 Dresden, Germany.
†Deceased.

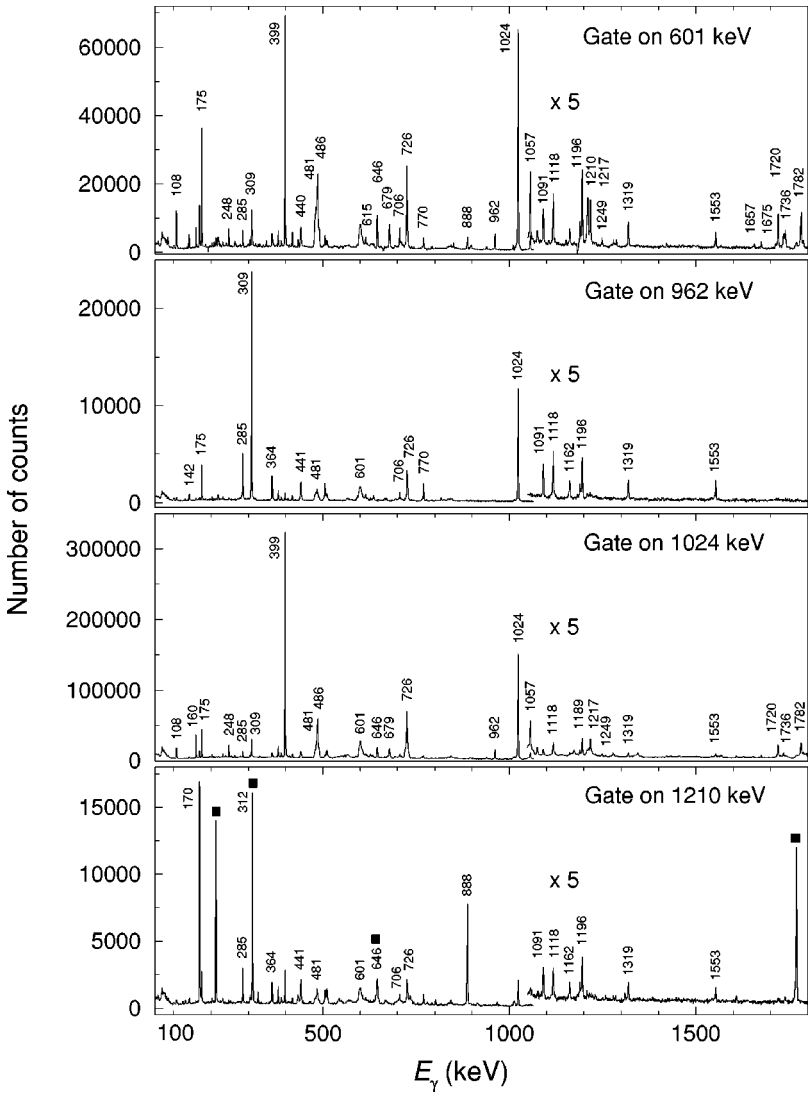

FIG. 1. Examples of background-corrected γ-γ coincidence spectra. Peaks marked with their energies are assigned to ^{87}Y. Peaks marked with squares in the bottom graph belong to ^{88}Y.

Experimental intensities W can be extracted from E_γ–E_γ coincidence matrices of selected detector pairs. The six Ge detectors of the OSIRIS CUBE are placed at angles of 45°, 90°, and 135° to the beam direction, two at each angle. Using the symmetry relation $W(\theta_1,\theta_2,\phi)=W(180°-\theta_1,180°-\theta_2,\phi)$ [14] there are eight detector pairs corresponding to $\theta_1=45°$, $\theta_2=90°$, $\phi=90°$. Consequently, the γ-γ coincidence events were sorted into eight separate E_γ–E_γ matrices that are related to each of these detector pairs. To reduce the influence of the energy dependence of the time signals on the γ-γ coincidence efficiency of the different detector pairs a wide time interval of 400 ns was used. Coincidence spectra were extracted by setting gates on certain peak and background intervals in the (45°,90°) and the transposed (90°,45°) matrices. These spectra were corrected for the energy-dependent efficiencies of the two detectors involved. To utilize the full statistics all eight spectra related to a certain peak or background gate at one angle combination were added up. DCO ratios were then obtained from peak intensities in the background-corrected sum spectra.

Mixing ratios δ were deduced from a comparison of the experimental DCO ratios with theoretical values calculated for certain initial and final spins as a function of $\arctan\delta$ with the computer code KORREL [15]. In these calculations the knowledge of the width σ of the Gaussian distribution assumed for the population of the magnetic substates of an incompletely aligned state with spin J_i is necessary. Since this quantity could not be determined from the experiment, a spin-dependent variation of σ/J_i has been taken into account within the range of $\sigma/J_i\approx 0.28-0.32$ that was empirically proved for compound nucleus reactions [16]. DCO ratios and mixing ratios obtained for transitions in ^{87}Y are listed in Table I. The experimental DCO ratios of three transitions are smaller than the smallest values predicted by the calculations, so that no mixing ratio could be derived from this comparison. Possible reasons for this discrepancy might be that assumptions used in the calculations are not valid for these transitions, or that the transitions are contaminated. For some transitions considered to have multipolarity $E1$ nonvanishing mixing ratios have been deduced. Since large $M2$ admixtures are unlikely, the absolute δ values may be close to their lower margins of error. These are smaller than 0.1 corresponding to $M2$ admixtures of less than 1%.

TABLE I. γ transitions assigned to ^{87}Y.

E_γ [a] (keV)	I_γ [b]	R_{DCO} [c]	E_γ^{GATE} [d] (keV)	δ [e]	$\sigma\lambda$ [f]	J_i^π [g]	J_f^π [h]	E_i [i] (keV)
27.0						$17/2^-$	$15/2^-$	2676
107.5	4.0(4) [j]	0.24(6) [m]	1024		($E1$)	$29/2^{(-)}$	$27/2^{(+)}$	5935
142.2	0.7(2) [j]	0.68(26)	1024		$M1/E2$	$23/2^{(-)}$	$21/2^{(-)}$	3909
159.8	6.0(3)	0.59(3)	1024	0.25(15)	$M1/E2$	$19/2^+$	$21/2^+$	2988
169.9	13.3(6) [j]	0.59(6)	1024	–0.15(25)	$M1$	$15/2^-$	$13/2^-$	2650
174.9	10.4(6) [j]	0.59(3)	1024	–0.20(12)	$M1$	$29/2^{(-)}$	$27/2^{(-)}$	5935
		0.92(7)	962					
247.9	3.4(3) [j]	0.97(5)	1024	0.19(11)	($E1$)	$17/2^-$	$17/2^+$	2676
264.3	0.7(1) [j]	0.64(7)	399	–0.20(20)	($E1$)	$27/2^{(-)}$	$25/2^+$	5760
285.4	5.5(3)	0.96(7)	1024	0.07(28)	$M1$	$17/2^-$	$17/2^-$	2962
		1.42(12)	962					
309.1	17(2) [j]	0.62(2)	1024	–0.08(8)	$M1$	$17/2^-$	$15/2^-$	2676
		0.90(3)	962					
312.3	2.2(2) [j]	0.52(8)	1024	–0.4(3)	$M1/E2$	$17/2^-$	$15/2^-$	2962
331.7	0.4(1) [j]					$27/2^{(+)}$	$25/2^+$	5827
364.1	3.9(3)	0.61(6)	1024	–0.15(20)	$M1$	$21/2^{(-)}$	$19/2^{(-)}$	3767
380.8	234(10)					$9/2^+$	$1/2^-$	381
399.0	100(2)	1.01(2)	1024		$E2$	$21/2^+$	$17/2^+$	2828
439.7	0.8(2) [j]	0.73(4) [n]	1024	0.10(10) [n]	$M1$	$27/2^{(-)}$	$25/2^{(-)}$	5760
440.9	3.8(3) [j]				($M1$)	$19/2^{(-)}$	$17/2^-$	3403
441.1	3.0(3) [j]				($M1$)	$13/2^-$	$(11/2^-)$	2480
481.1	14(2) [j,k]	0.65(10)	1024	–0.10(15)	$M1$	$33/2^{(-)}$	$31/2^{(-)}$	7017
486.4	41(3) [j,k]	0.60(6)	1024	–0.16(20)	$M1$	$25/2^+$	$23/2^+$	4040
506.4	3.3(2) [j]					$23/2^{(-)}$	$19/2^{(-)}$	3909
531.5	0.5(2) [j]					$27/2^{(-)}$	$25/2^{(-)}$	5760
558.7	2.1(2) [j]					$19/2^+$	$17/2^+$	2988
569.0	1.3(3) [j]					$25/2^+$	$25/2^+$	4610
601.0	29(2) [j,k]	0.76(6)	399	0.14(14)	$M1$	$31/2^{(-)}$	$29/2^{(-)}$	6536
615.0	2.2(4) [j]					$29/2^{(-)}$	$25/2^{(-)}$	5935
633.3	4.7(5) [j]					$(11/2^-)$	$13/2^+$	2038
646.0	8.3(6) [j]	0.53(6)	1024	–0.5(4)	($E1$)	$29/2^{(-)}$	$27/2^+$	5935
678.8	11(2) [j,k]	0.32(2) [m]	399		$M1/E2$	$27/2^+$	$25/2^+$	5289
706.3	4.6(5)					$29/2^{(-)}$	$25/2^{(-)}$	5935
725.8	59(5) [j,k]	0.59(6)	399	–0.20(22)	$M1$	$23/2^+$	$21/2^+$	3554
726.4	7.5(6)	0.70(5)	962	0.09(11)	($M1$)	$19/2^{(-)}$	$17/2^-$	3403
770.5	6.2(7)	0.58(5)	1024	–0.19(17)	($M1$)	$19/2^{(-)}$	$17/2^-$	3446
793.5	6.6(4)					$5/2^-$	$1/2^-$	794
835.8	1.0(1) [j]						$5/2^-$	1629
888.2	11.7(6)					$13/2^-$	$11/2^+$	2480
940.1	0.9(1) [j]	0.52(6)	1024	–0.8(5)	$M1/E2$	$25/2^+$	$23/2^+$	5496
962.3	18.2(9)	0.65(2)	1024	0.03(7)	$E1$	$15/2^-$	$13/2^+$	2367
974.5	0.7(1)					$(9/2^-)$	$5/2^-$	1768
1011.4	2.4(10)	0.9(5)	1024		($E1$)	$23/2^{(-)}$	$23/2^+$	4565
1023.6	159(19) [l]	1.01(4) [o]				$13/2^+$	$9/2^+$	1405
1023.6	129(7) [j]		1024		$E2$	$17/2^+$	$13/2^+$	2429
1040.2	0.3(1) [j]					$(13/2^-)$	$(9/2^-)$	2808
1056.8	12(3) [j,k]	0.70(8)	1024	0.04(18)	$M1$	$25/2^+$	$23/2^+$	4610
1090.6	2.6(3) [j]	1.49(20)	962		$E2$	$21/2^{(-)}$	$17/2^-$	3767
1117.6	5.9(4)	1.02(7)	1024		$E2$	$23/2^{(-)}$	$19/2^{(-)}$	4565
		1.40(10)	962					
1161.7	1.8(2)					$23/2^{(-)}$	$19/2^{(-)}$	4565
1189.1	1.4(2)	0.87(18)	399		($E1$)	$25/2^{(-)}$	$25/2^+$	5229

TABLE I. (*Continued*).

E_γ [a] (keV)	I_γ [b]	R_{DCO} [c]	E_γ^{GATE} [d] (keV)	δ [e]	$\sigma\lambda$ [f]	J_i^π [g]	J_f^π [h]	E_i [i] (keV)
1195.6	5.7(4) [j]	1.45(13)	962		$(E2)$	$27/2^{(-)}$	$23/2^{(-)}$	5760
1209.9	26.6(12)					$11/2^+$	$9/2^+$	1591
1214.9	0.9(1) [j]						$5/2^-$	2008
1217.4	5.9(8) [j]	0.45(4)	1024	−1.0(3)	$M1/E2$	$27/2^{(+)}$	$25/2^+$	5827
1249.0	1.3(2) [j]	0.21(4) [m]	1024		$M1/E2$	$27/2^+$	$25/2^+$	5289
1319.4	1.8(2) [j]	0.75(11)	1024	0.14(22)	$M1$	$25/2^{(-)}$	$23/2^{(-)}$	5229
		1.17(16)	962					
1553.0	3.5(5) [j,k]	1.37(15)	962		$(E2)$	$25/2^{(-)}$	$21/2^{(-)}$	5320
1568.2	2.1(3)	1.99(23)	160		$(E2)$	$23/2^+$	$19/2^+$	4556
1656.8	2.3(2)					$(11/2^-)$	$9/2^+$	2038
1675.1	1.0(1)	0.56(9)	1024	−0.27(27)	$(E1)$	$25/2^{(-)}$	$23/2^+$	5229
1720.0	5.4(6)	0.61(3)	1024	−0.14(10)	$(E1)$	$27/2^{(-)}$	$25/2^+$	5760
1727.6	1.3(4)					$23/2^+$	$21/2^+$	4556
1735.8	2.3(3) [j]					$27/2^+$	$23/2^+$	5289
1782.4	10(2) [j,k]	1.03(13)	1024		$E2$	$25/2^+$	$21/2^+$	4610
1787.8	2.6(4)					$27/2^{(+)}$	$25/2^+$	5827
1942.2	1.1(1)	0.43(6)	1024	−0.8(3)	$M1/E2$	$25/2^+$	$23/2^+$	5496

[a]Transition energy. The error is in the range of (0.1–0.5) keV.

[b]Relative intensity of the γ ray normalized to $I_\gamma=100$ of the $21/2_1^+\rightarrow 17/2_1^+$ transition at 399.0 keV. This value represents the quantity A_0 of the expression $W(\theta)=A_0[1+A_2P_2(\cos\theta)]$ and was deduced from intensities in singles spectra measured at $\theta=45°$ and 90°. If the transition might be influenced by other lines the intensity was deduced from coincidence spectra (see j).

[c]DCO ratio $R_{DCO}=W(90°,45°,90°)/W(45°,90°,90°)$.

[d]Energy of the gating transition used for the determination of the DCO ratio.

[e]Mixing ratio $\delta=\langle J_f\|\hat{M}(\lambda=2)\|J_i\rangle/\langle J_f\|\hat{M}(\lambda=1)\|J_i\rangle$ deduced from the DCO ratio. The sign of δ is chosen such that it is consistent with the sign of δ values deduced from angular distribution coefficients [19]. In the case of more than one solution the smaller absolute δ value is given. The error includes the error of the DCO ratio and a certain variation of the width σ/J_i (see Sec. II A).

[f]Multipolarity compatible with the DCO ratio and the deexcitation mode. The notation $M1/E2$ is given, if the $E2$ admixture derived from the mean δ value is greater than 5%.

[g]Spin and parity of the initial state.

[h]Spin and parity of the final state.

[i]Energy of the initial state.

[j]Intensity deduced from coincidence spectra including γ-γ coincidence events of all detector pairs.

[k]Doppler-shifted portion of the intensity taken into account.

[l]This value is the difference between the intensity of the unresolved doublet and the intensity of the $17/2^+\rightarrow 13/2^+$ transition obtained from coincidence spectra.

[m]This value is smaller than the minimum value predicted by the calculations (see Sec. II A). A mixing ratio could not be derived.

[n]Combined value derived for the 439.7-440.9-441.1 keV triplet.

[o]Combined value derived for the 1023.6 keV doublet.

B. Lifetimes

Mean lifetimes were determined from Doppler shifts of γ rays observed in coincidence spectra at angles of 45° and 135° to the beam direction using the DSA method. These coincidence spectra were extracted from two E_γ–E_γ matrices containing coincidence events of all Ge detector pairs that include one detector at 45° or 135°, respectively. The lifetimes were deduced from a comparison of experimental with calculated line shapes. The velocity distributions of the emitting nuclei were calculated with a Monte Carlo code taking into account reactions at different depths in the target, the kinematics of the reaction and the slowing down and deflection of the recoils [17]. For the slowing down the cross sections given in Ref. [18] were used with correction factors of $f_e=0.9$ and $f_n=0.7$ for the electronic and nuclear stopping powers, respectively [1]. The sidefeeding times were neglected for excitation energies above 11 MeV. This value represents roughly the maximum excitation energy of the final nucleus $E^*=E^{CM}_{^{11}B}+Q-4E_n$ with a value of $Q=-18.4$ MeV and a mean energy of the emitted neutrons of $E_n\approx 2.5$ MeV. With decreasing excitation energy an increase of the sidefeeding times according to $\tau_{sf}=(11-E/\mathrm{MeV})\times 0.03$ ps was assumed [1]. Examples of the line-shape analysis are shown in Fig. 2. The lifetimes obtained from this analysis are given in Table II.

III. THE LEVEL SCHEME OF ^{87}Y

The level scheme of ^{87}Y deduced from the present experiment is shown in Fig. 3. It results from the γ-γ coincidence relations and the γ-ray intensities. The spin and parity assignments are based on DCO ratios of the γ rays as well as

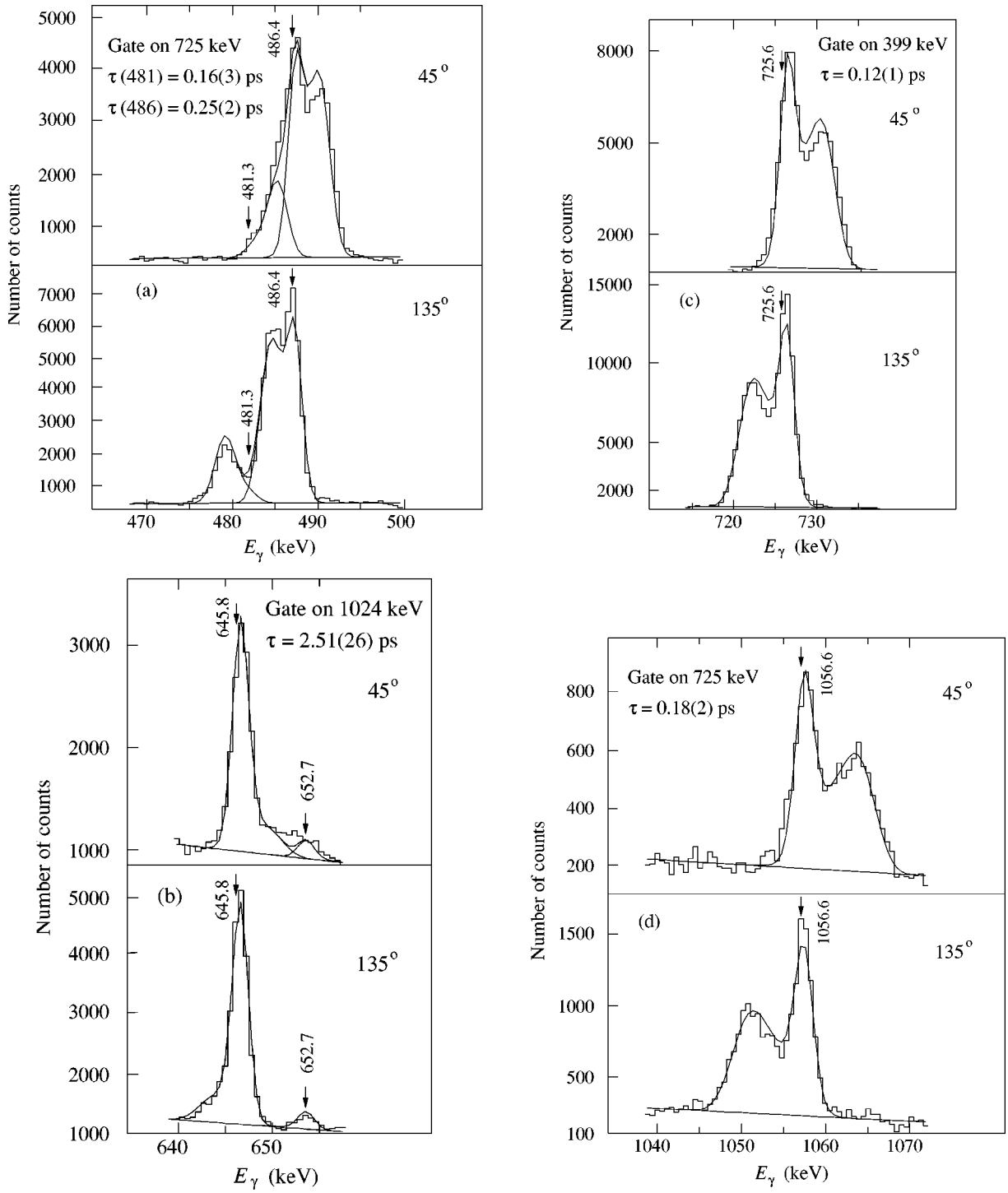

FIG. 2. Examples of the line-shape analysis using the DSA method. Lifetimes were deduced from a joint fit of calculated to experimental line shapes at the complementary observation angles of 45° and 135°. Feeding corrections are included. The values of energies, lifetimes, and their errors are results of the presented fits.

on deexcitation modes and lifetimes. Extensions and alterations of the level scheme with respect to previous work are discussed in the following section.

The sequence of positive-parity yrast states built on the $9/2^+$ isomeric state (τ=19.3 h) has been known up to the $25/2^+$ state at 4040 keV from Ref. [5]. In that work a $(27/2^+)$ state deexciting via a 174.9 keV transition to the $25/2^+$ yrast state was proposed. We do not confirm this placement of the 174.9 keV transition and consider the state at 5289 keV as the $27/2^+$ yrast state that populates the $23/2^+$ and $25/2^+$ yrast states via 1735.8 and 1249.0 keV transitions, respectively. Above the $27/2^+$ state we tentatively propose a change of the parity within the sequence of yrast states that is discussed below.

In Refs. [5,6] a cascade of 159.8 and 107.5 keV transitions was placed on top of the $21/2^+$ state and assignments of $23/2^+$ and $25/2^+$ were made for the corresponding levels at 2988 and 3094 keV, respectively, which would be yrast

TABLE II. Mean lifetimes of states in ^{87}Y.

E_i (keV) [a]	E_γ (keV) [b]	τ (ps) [c]
3554	725.8	0.12(3)
4040	486.4	0.25(6)
4610	1056.8	0.18(5)
5289	678.8	0.14(4)
5760	1720.0	>3
5935	646.0	2.6(5)
6536	601.0	0.26(5)
7017	481.1	0.16(4)

[a]Level energy.

[b]Energy of the γ ray used for the line-shape analysis in connection with the DSA method.

[c]Mean lifetime. The error in parentheses includes the statistical error, uncertainties of feeding times and feeding intensities and a 10% uncertainty of the nuclear and electronic stopping power.

states in that case. However, this is not consistent with the small intensities of the 159.8 and 107.5 keV transitions compared with those of the 725.8 and 486.4 keV transitions deexciting the $23/2^+$ and $25/2^+$ states at 3554 and 4040 keV, respectively. Moreover, the states at 2988 and 3094 keV do not fit the systematic behavior of $23/2^+$ and $25/2^+$ yrast states in the chain of $N=48$ isotones [1]. Therefore, we propose spin and parity $19/2^+$ for the 2988 keV level. This assignment is compatible with the DCO ratio of the 159.8 keV transition and is supported by the observation of a 558.7 keV transition depopulating the state at 2988 keV to the $17/2^+$ yrast state. We do not confirm the placement of the 107.5 keV transition on top of the 2988 keV level as given in Refs. [5,6]. Instead, we infer $23/2^+$ and $25/2^+$ states at 4556 and 5496 keV, respectively, from the observation of a cascade of transitions at 1568.2 and 940.1 keV as well as of 1727.6 and 1942.2 keV transitions in the present experiment.

The 1056.8 keV transition deexciting a level at 4610 keV has been known from previous work [5]. We have observed two further transitions depopulating this level and a 678.8 keV transition feeding it from the $27/2^+$ yrast state. Based on DCO ratios and the short lifetime we assign spin and parity $25/2^+$ to the 4610 keV level. On top of this we have found a $27/2^{(+)}$ state at 5827 keV. The previously known 107.5 keV transition (see above discussion) is found to populate this state.

The cascade of 888.2, 169.9, 312.3, 440.9, and 364.1 keV transitions on top of the $11/2^+$ state at 1591 keV was already observed in Ref. [5]. The levels at 2480 and 2962 keV were considered to correspond to levels at 2486 and 2958 keV, respectively, identified in the ^{89}Y(p,t) study [4]. In that work negative parity was inferred from a distorted-wave Born approximation analysis for those levels. Based on this assumption negative parity has been proposed also for the 2650 keV level and tentatively for the 3403 and 3767 keV levels [20]. We have observed a 1553.0 keV transition on top of this sequence and suggest the assignment $25/2^{(-)}$ for the level at 5320 keV. The assignment of negative parity for the states at 3767 and 5320 keV is supported by their deexcitation via $\Delta J=2$ transitions: in the case of a parity change these would have the rather unlikely multipolarity $M2$. The levels at 2367, 2676, and 3446 keV have been known from Ref. [5]. In that work a 27.0 keV transition linking the 2676 with the 2650 keV level was introduced. We confirm the existence of such a transition indirectly by the observation of coincidences of the 169.9 and 770.5 keV transitions. The levels at 2367 and 2676 keV were also considered to correspond to negative-parity states found in the ^{89}Y(p,t) study [4]. We found further levels at 3909, 4565, and 5229 keV where negative parity is tentatively assumed, too.

In the present study we have discovered the yrast states with $J=29/2$, $31/2$, and $33/2$ at 5935, 6536, and 7017 keV, respectively. The previously known 174.9 keV transition (see above) is found in the present experiment to depopulate the yrast state with $J=29/2$ to a state with $J=27/2$ at 5760

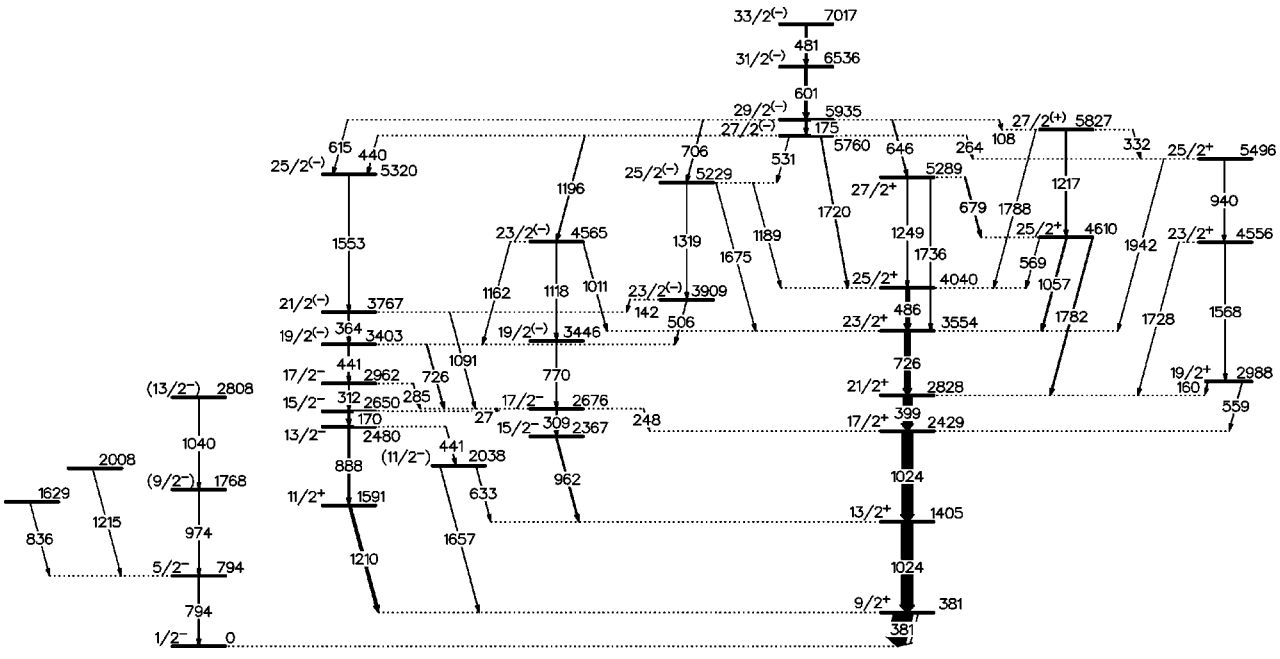

FIG. 3. Level scheme of ^{87}Y deduced from the present experiment.

keV. We propose tentatively negative parity for all these states: if they had positive parity, strengths of $B(M2)\approx 140$ W.u. and $B(M2)\approx 900$ W.u. would result from the present lifetime measurements for the 1195.6 keV transition deexciting the $J=27/2$ state at 5760 keV and for the 615.0 and 706.3 keV transitions deexciting the $J=29/2$ state, respectively. Such $M2$ strengths can be excluded as they are up to three orders of magnitude greater than values expected in this mass region [21]. However, the assignment of negative parity includes one exceptional transition strength, too. Whereas usual strengths of $B(E1)<6\times 10^{-4}$ W.u. are deduced from the present lifetime measurements for the 264.3 and 1720.0 keV transitions depopulating the $27/2^{(-)}$ state and the 646.0 keV transition deexciting the $29/2^{(-)}$ state, the 107.5 keV transition linking the $29/2^{(-)}$ and $27/2_2^{(+)}$ states has a strength of $B(E1)=2\times 10^{-2}$ W.u. This value exceeds the largest values compiled for this mass region in Ref. [21] by a factor of about 30, but is only by a factor of about 8 larger than $E1$ transition strengths observed in the isotope ^{89}Y [22,23]. This problem could be solved by assuming multipolarity $M1/E2$ for the 107.5 keV transition. In this case the level at 5827 keV would have negative parity and the 1217.4 and 1787.8 keV transitions would be $E1$ transitions. Since transition strengths of these transitions could not be deduced, this assumption cannot be excluded. However, the deexcitation modes of the 5827 keV level may support the assignment of positive parity.

The $5/2^-$ state at 794 keV has been known from previous work [5]. We found two levels at 1768 and 2808 keV forming a sequence with the $5/2^-$ state. In addition, two levels at 1629 and 2008 keV feeding the $5/2^-$ state are proposed.

IV. SHELL-MODEL INTERPRETATION

The nucleus ^{87}Y has one proton above the level gap at $Z=38$ and two neutron holes in the $N=50$ shell. The level structure of this nucleus displays characteristics of few-particle excitations in a nearly spherical nucleus: the level sequences are multipletlike and comprise only weak or no $E2$ but strong $M1$ transitions. The interpretation of these structures within the framework of the shell model is presented in the following.

A. Shell-model calculations

Shell-model studies of nuclei with $N=48$ and $Z>38$ have mainly been carried out so far in a restricted model space generated out of the $1p_{1/2}$ and $0g_{9/2}$ orbitals for protons as well as neutrons [24–28] and with empirical effective interactions [24,29,30]. Most of the levels with low or moderate spin in the nuclei ^{86}Sr, ^{87}Y, ^{88}Zr, ^{89}Nb, and ^{90}Mo [24,27,28,31] could be described within that model space. However, excitations of $0f_{5/2}$ or $1p_{3/2}$ protons may contribute to the configurations of high-spin states as observed in the present study.

The model space used in our calculations includes the active proton orbitals $\pi(0f_{5/2},1p_{3/2},1p_{1/2},0g_{9/2})$ and neutron orbitals $\nu(1p_{1/2},0g_{9/2})$ relative to a hypothetic ^{66}Ni core. Since an empirical Hamiltonian for this model space is not available up to now, various empirical Hamiltonians have been combined with results of schematic nuclear interactions applying the surface δ interaction. Details of this procedure are described in Refs. [32,33]. The effective interaction in the proton shells was taken from Ref. [34]. In that work the residual interaction and the single-particle energies of the proton orbitals were deduced from a least-squares fit to 170 experimental level energies in $N=50$ nuclei with mass numbers between 82 and 96. The data given in Ref. [24] have been used for the proton-neutron interaction between the $\pi(1p_{1/2},0g_{9/2})$ and the $\nu(1p_{1/2},0g_{9/2})$ orbitals. These data were derived from an iterative fit to 95 experimental level energies of $N=48$, 49, and 50 nuclei. The matrix elements of the neutron-neutron interaction of the $\nu(1p_{1/2},0g_{9/2})$ orbitals have been assumed to be equal to the isospin $T=1$ component of the proton-neutron interaction given in Ref. [24]. For the $(\pi 0f_{5/2},\nu 0g_{9/2})$ residual interaction the matrix elements proposed in Ref. [35] have been used.

The single-particle energies relative to the ^{66}Ni core have been derived from the single-particle energies of the proton orbitals given in Ref. [34] with respect to the ^{78}Ni core and from the neutron single-hole energies of the $1p_{1/2},0g_{9/2}$ orbitals [24]. The transformation of these single-particle energies to those relative to the ^{66}Ni core has been performed [36] on the basis of the effective residual interactions given above. The obtained values are $\epsilon^{\pi}_{f_{5/2}}=-9.106$ MeV, $\epsilon^{\pi}_{p_{3/2}}=-9.033$ MeV, $\epsilon^{\pi}_{p_{1/2}}=-4.715$ MeV, $\epsilon^{\pi}_{g_{9/2}}=-0.346$ MeV, $\epsilon^{\nu}_{p_{1/2}}=-7.834$ MeV, $\epsilon^{\nu}_{g_{9/2}}=-6.749$ MeV. These single-particle energies and the corresponding values for the strengths of the residual interactions have been used to calculate level energies as well as $M1$ and $E2$ transition strengths. For the latter, effective g factors of $g_s^{\rm eff}=0.7g_s^{\rm free}$ and effective charges of $e_\pi=1.72e, e_\nu=1.44e$ [37], respectively, have been applied.

The nucleus ^{87}Y has 11 protons and 10 neutrons in the considered configuration space. To make the calculations feasible a truncation of the occupation numbers has been applied: at least one but at most four protons are allowed to occupy the $(1p_{1/2},0g_{9/2})$ subshell. Two of the neutrons are assumed to occupy the $1p_{1/2}$ orbital while the remaining eight appear in the $0g_{9/2}$ orbital. With these restrictions a configuration space with dimensions smaller than 9200 has been obtained. The calculations were carried out with the code RITSSCHIL [38].

To investigate structural differences between states in ^{87}Y and in the isotone ^{85}Rb we have carried out shell-model calculations for the latter nucleus, too. The nucleus ^{85}Rb has 37 protons, i.e., one proton hole in the $(0f_{5/2},1p_{3/2})$ subshell. In the calculations the truncation of the number of excitations in the $\pi(1p_{1/2},0g_{9/2})$ subshell has been chosen so that it is compatible with the calculations for ^{87}Y, i.e., a maximum of three or four protons is allowed to occupy this subshell for positive-parity or negative-parity states, respectively.

B. Results

Calculated level energies of states in ^{87}Y are compared with experimental ones in Fig. 4. The main configurations of the shell-model states are listed in Table III; experimental and calculated transition strengths are compiled in Table IV.

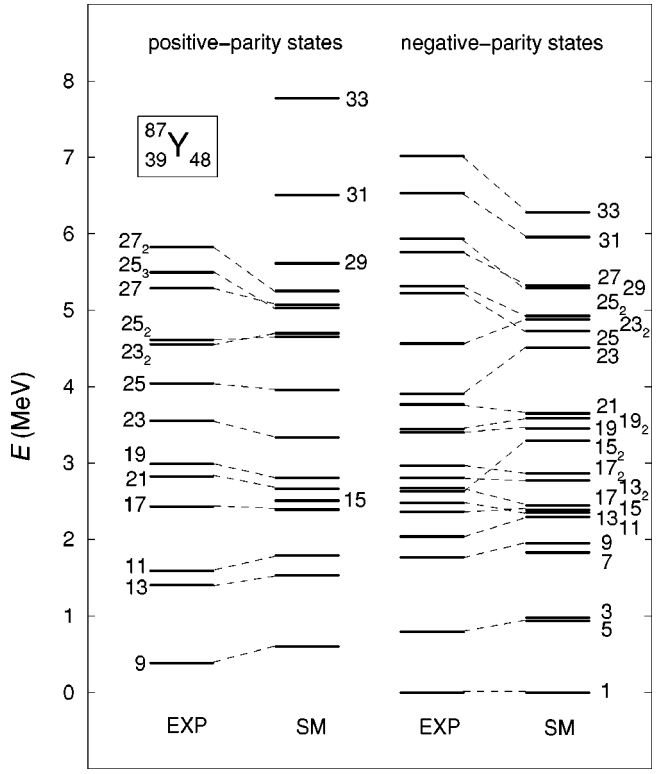

FIG. 4. Comparison of experimental with calculated level energies of states in ^{87}Y. Spins are given as $2J$.

It can be seen that the calculated level energies and transition strengths are in good agreement with the experiment.

The positive-parity yrast states with $9/2 \leqslant J \leqslant 25/2$ are characterized by the coupling of one $0g_{9/2}$ proton to the two neutron holes in the $0g_{9/2}$ orbital. The sequence of the experimental yrast states, in particular that of the $11/2_1^+$, $13/2_1^+$ and the $19/2_1^+$, $21/2_1^+$ states, is reproduced in the calculations. Moreover, the calculated $B(E2)$ and $B(M1)$ values of the transitions deexciting the $21/2_1^+$, $23/2_1^+$, $25/2_1^+$, and $25/2_2^+$ states are consistent with the experimental ones (see Table IV). To create a $27/2^+$ state the breakup of a pair of nucleons is necessary. In the main configuration of the $27/2_1^+$, $29/2_1^+$, and $31/2_1^+$ states a pair of $0f_{5/2}$ protons is broken and one proton lifted to the $1p_{1/2}$ orbital. This structural change from seniority $v=3$ to $v=5$ above the $25/2_1^+$ states reflects in a relatively large spacing and a small $B(M1)$ transition strength between the $25/2_1^+$ and $27/2_1^+$ states, both found in the calculation as well as in the experiment (see Fig. 4 and Table IV). The creation of a $33/2^+$ state requires the breakup of an additional pair of nucleons. The main configuration of this $v=7$ state is dominated by two $0f_{5/2}$ proton holes and three protons in the $0g_{9/2}$ orbital, coupled to the two $0g_{9/2}$ neutron holes.

The $1/2^-$ ground state contains mainly one $1p_{1/2}$ proton. Its coupling to the two $0g_{9/2}$ neutron holes predominates in the lowest-lying negative-parity states with $3/2 \leqslant J \leqslant 17/2$ except for the $5/2^-$ and $7/2^-$ states which are described by a

TABLE III. Main components of wave functions of states in ^{87}Y.

J^π	Configuration[a]		v[b]	A[c]	J^π	Configuration[a]		v[b]	A[c]
$9/2_1^+$	$\pi 0g_{9/2}^1$	$\nu(0g_{9/2}^{-2})_0$	1	49	$1/2_1^-$	$\pi 1p_{1/2}^1$	$\nu(0g_{9/2}^{-2})_0$	1	80
$11/2_1^+$	$\pi 0g_{9/2}^1$	$\nu(0g_{9/2}^{-2})_2$	3	31	$3/2_1^-$	$\pi 1p_{1/2}^1$	$\nu(0g_{9/2}^{-2})_2$	3	43
$13/2_1^+$	$\pi 0g_{9/2}^1$	$\nu(0g_{9/2}^{-2})_2$	3	49		$\pi 1p_{3/2}^{-1}$	$\nu(0g_{9/2}^{-2})_0$	1	31
$15/2_1^+$	$\pi 0g_{9/2}^1$	$\nu(0g_{9/2}^{-2})_4$	3	26	$5/2_1^-$	$\pi[0f_{5/2}^{-1}(0g_{9/2}^2)_0]$	$\nu(0g_{9/2}^{-2})_0$	1	20
$17/2_1^+$	$\pi 0g_{9/2}^1$	$\nu(0g_{9/2}^{-2})_4$	3	41	$7/2_1^-$	$\pi[0f_{5/2}^{-1}(0g_{9/2}^2)_0]$	$\nu(0g_{9/2}^{-2})_2$	3	21
$19/2_1^+$	$\pi 0g_{9/2}^1$	$\nu(0g_{9/2}^{-2})_8$	3	45	$9/2_1^-$	$\pi 1p_{1/2}^1$	$\nu(0g_{9/2}^{-2})_4$	3	62
$21/2_1^+$	$\pi 0g_{9/2}^1$	$\nu(0g_{9/2}^{-2})_8$	3	43	$11/2_1^-$	$\pi 1p_{1/2}^1$	$\nu(0g_{9/2}^{-2})_6$	3	74
$23/2_1^+$	$\pi 0g_{9/2}^1$	$\nu(0g_{9/2}^{-2})_8$	3	57	$13/2_1^-$	$\pi 1p_{1/2}^1$	$\nu(0g_{9/2}^{-2})_6$	3	78
$23/2_2^+$	$\pi[1p_{3/2}^{-1}1p_{1/2}^1 0g_{9/2}^1]_{11/2}$	$\nu(0g_{9/2}^{-2})_8$	5	30	$13/2_2^-$	$\pi[0f_{5/2}^{-1}(0g_{9/2}^2)_6]$	$\nu(0g_{9/2}^{-2})_0$	3	24
$25/2_1^+$	$\pi 0g_{9/2}^1$	$\nu(0g_{9/2}^{-2})_8$	3	55	$15/2_1^-$	$\pi 1p_{1/2}^1$	$\nu(0g_{9/2}^{-2})_8$	3	80
$25/2_2^+$	$\pi[1p_{3/2}^{-1}1p_{1/2}^1 0g_{9/2}^1]_{13/2}$	$\nu(0g_{9/2}^{-2})_8$	5	25	$15/2_2^-$	$\pi[0f_{5/2}^{-1}(0g_{9/2}^2)_6]$	$\nu(0g_{9/2}^{-2})_0$	3	11
	$\pi[1p_{3/2}^{-1}1p_{1/2}^1 0g_{9/2}^1]_{11/2}$	$\nu(0g_{9/2}^{-2})_8$	5	22	$17/2_1^-$	$\pi 1p_{1/2}^1$	$\nu(0g_{9/2}^{-2})_8$	3	81
$25/2_3^+$	$\pi[0f_{5/2}^{-1}1p_{1/2}^1 0g_{9/2}^1]_{13/2}$	$\nu(0g_{9/2}^{-2})_8$	5	33	$17/2_2^-$	$\pi[0f_{5/2}^{-1}(0g_{9/2}^2)_8]$	$\nu(0g_{9/2}^{-2})_0$	3	30
$27/2_1^+$	$\pi[0f_{5/2}^{-1}1p_{1/2}^1 0g_{9/2}^1]_{13/2}$	$\nu(0g_{9/2}^{-2})_8$	5	42	$19/2_1^-$	$\pi[0f_{5/2}^{-1}(0g_{9/2}^2)_8]$	$\nu(0g_{9/2}^{-2})_0$	3	33
$27/2_2^+$	$\pi[1p_{3/2}^{-1}1p_{1/2}^1 0g_{9/2}^1]_{13/2}$	$\nu(0g_{9/2}^{-2})_8$	5	38	$19/2_2^-$	$\pi[1p_{3/2}^{-1}(1p_{1/2}^2)_0]$	$\nu(0g_{9/2}^{-2})_8$	3	60
	$\pi[1p_{3/2}^{-1}1p_{1/2}^1 0g_{9/2}^1]_{11/2}$	$\nu(0g_{9/2}^{-2})_8$	5	25	$21/2_1^-$	$\pi[0f_{5/2}^{-1}(0g_{9/2}^2)_0]$	$\nu(0g_{9/2}^{-2})_8$	3	31
$29/2_1^+$	$\pi[0f_{5/2}^{-1}1p_{1/2}^1 0g_{9/2}^1]_{13/2}$	$\nu(0g_{9/2}^{-2})_8$	5	48	$23/2_1^-$	$\pi[0f_{5/2}^{-1}(0g_{9/2}^2)_8]_{19/2}$	$\nu(0g_{9/2}^{-2})_2$	5	30
	$\pi[0f_{5/2}^{-1}1p_{1/2}^1 0g_{9/2}^1]_{15/2}$	$\nu(0g_{9/2}^{-2})_8$	5	23	$23/2_2^-$	$\pi[1p_{3/2}^{-1}(0g_{9/2}^2)_6]_{11/2}$	$\nu(0g_{9/2}^{-2})_6$	5	6
$31/2_1^+$	$\pi[0f_{5/2}^{-1}1p_{1/2}^1 0g_{9/2}^1]_{15/2}$	$\nu(0g_{9/2}^{-2})_8$	5	73	$25/2_1^-$	$\pi[0f_{5/2}^{-1}(0g_{9/2}^2)_2]_{9/2}$	$\nu(0g_{9/2}^{-2})_8$	5	50
$33/2_1^+$	$\pi[(0f_{5/2}^{-2})_2(0g_{9/2}^3)_{21/2}]_{25/2}$	$\nu(0g_{9/2}^{-2})_4$	7	13	$25/2_2^-$	$\pi[0f_{5/2}^{-1}(0g_{9/2}^2)_8]_{17/2}$	$\nu(0g_{9/2}^{-2})_4$	5	18
					$27/2_1^-$	$\pi[0f_{5/2}^{-1}(0g_{9/2}^2)_8]_{17/2}$	$\nu(0g_{9/2}^{-2})_8$	5	22
					$29/2_1^-$	$\pi[0f_{5/2}^{-1}(0g_{9/2}^2)_4]_{13/2}$	$\nu(0g_{9/2}^{-2})_8$	5	19
					$31/2_1^-$	$\pi[0f_{5/2}^{-1}(0g_{9/2}^2)_8]_{17/2}$	$\nu(0g_{9/2}^{-2})_8$	5	22
					$33/2_1^-$	$\pi[0f_{5/2}^{-1}(0g_{9/2}^2)_6]_{17/2}$	$\nu(0g_{9/2}^{-2})_8$	5	39

[a]Main contribution to the wave function. The second strongest contribution is given if it is greater than 20%.
[b]Seniority.
[c]Amount of the contribution in percent.

TABLE IV. Experimental and calculated transition strengths in ^{87}Y.

E_γ (keV)	J_i^π	J_f^π	$\sigma\lambda$	$B(\sigma\lambda)_{EXP}$ [a] (W.u.)	$B(\sigma\lambda)_{SM}$ [b] (W.u.)
399.0	$21/2_1^+$	$17/2_1^+$	$E2$	4.5(3) [c]	6.2
725.8	$23/2_1^+$	$21/2_1^+$	$M1$	$0.69^{+0.23}_{-0.14}$	1.23
486.4	$25/2_1^+$	$23/2_1^+$	$M1$	$1.10^{+0.35}_{-0.21}$	0.87
1782.4	$25/2_2^+$	$21/2_1^+$	$E2$	$4.7^{+3.5}_{-1.9}$	4.6
1056.8	$25/2_2^+$	$23/2_1^+$	$M1$	$0.08^{+0.04}_{-0.03}$	0.04
569.0	$25/2_2^+$	$25/2_1^+$	$M1$	$0.05^{+0.03}_{-0.02}$	0.02
1735.8	$27/2_1^+$	$23/2_1^+$	$E2$	$2.5^{+2.0}_{-1.0}$	0.23
1249.0	$27/2_1^+$	$25/2_1^+$	$M1$	$0.010^{+0.009}_{-0.004}$	4×10^{-4}
678.8	$27/2_1^+$	$25/2_2^+$	$M1$	$0.55^{+0.27}_{-0.16}$	0.14
1195.6	$27/2_1^-$	$23/2_2^-$	$E2$	<2.4	0.3
531.5	$27/2_1^-$	$25/2_1^-$	$M1$	<0.004	0.07
439.7	$27/2_1^-$	$25/2_2^-$	$M1$	<0.01	0.03
1720.0	$27/2_1^-$	$25/2_1^+$	$E1$	$<2\times10^{-5}$	
264.3	$27/2_1^-$	$25/2_3^+$	$E1$	$<6\times10^{-4}$	
706.3	$29/2_1^-$	$25/2_1^-$	$E2$	$12.0^{+5.2}_{-3.6}$	5.0
615.0	$29/2_1^-$	$25/2_2^-$	$E2$	$11.4^{+6.1}_{-4.1}$	4.0
174.9	$29/2_1^-$	$27/2_1^-$	$M1$	$0.79^{+0.29}_{-0.20}$	1.12
646.0	$29/2_1^-$	$27/2_1^+$	$E1$	$(1.7^{+1.0}_{-0.3})\times10^{-4}$	
107.5	$29/2_1^-$	$27/2_2^+$	$E1$	$0.020^{+0.009}_{-0.006}$	
601.0	$31/2_1^-$	$29/2_1^-$	$M1$	$0.56^{+0.14}_{-0.09}$	1.40
481.1	$33/2_1^-$	$31/2_1^-$	$M1$	$1.78^{+0.60}_{-0.35}$	1.41

[a]Experimental reduced transition strengths derived from the lifetimes given in Table II and from the intensities in Table I. $E2$ admixtures of less than 5% are neglected. Weisskopf units are: 1 W.u.$(M1)=1.79\ \mu_N^2$; 1 W.u.$(E1)=1.27\ e^2$ fm^2; 1 W.u.$(E2)=22.90\ e^2$ fm^4.

[b]Calculated reduced transition strengths in Weisskopf units. Values of $g_s^{eff}=0.7g_s^{free}$ and $e_\pi=1.72e, e_\nu=1.44e$ have been used for the $B(M1)$ and $B(E2)$ values, respectively.

[c]Value taken from Ref. [6].

proton hole in the $0f_{5/2}$ orbital. In the main configuration of the lowest-lying negative-parity states with $19/2\leqslant J\leqslant 33/2$ the unpaired proton occupies the $0g_{9/2}$ orbital. In addition, a $0f_{5/2}$ proton pair is broken and one proton lifted to the $0g_{9/2}$ orbital. These three active protons couple to the two $0g_{9/2}$ neutron holes. The individual states are created by a recoupling of the spins of the involved nucleons (see Table III). This recoupling causes large $B(M1)$ strengths especially for the transitions between the $29/2_1^-$, $31/2_1^-$, and $33/2_1^-$ states which are compatible with the experimental values (see Table IV).

The calculation of $B(E1)$ values is not possible in the present model space. However, in a previous shell-model study of the isotope ^{89}Y, neutron excitations over the $N=50$ shell gap into the $\nu 0h_{11/2}$ orbital were considered that cause allowed $E1$ transitions [23]. To test whether the experimental $B(E1)$ values of up to 10^{-3} W.u. between states with $J\geqslant 21/2$ in ^{89}Y can be reproduced by such single-particle transitions, calculations were carried out using a restricted model space with configurations of the type $\pi[(0f_{5/2})^{6-n}(1p_{1/2}0g_{9/2})^{1+n}]\nu[(0g_{9/2})^{9-n}(1d_{5/2})(0h_{11/1})^n]$ with $n=0, 1$. The two-body matrix elements including the $\nu 1d_{5/2}$ and $\nu 0h_{11/2}$ orbitals

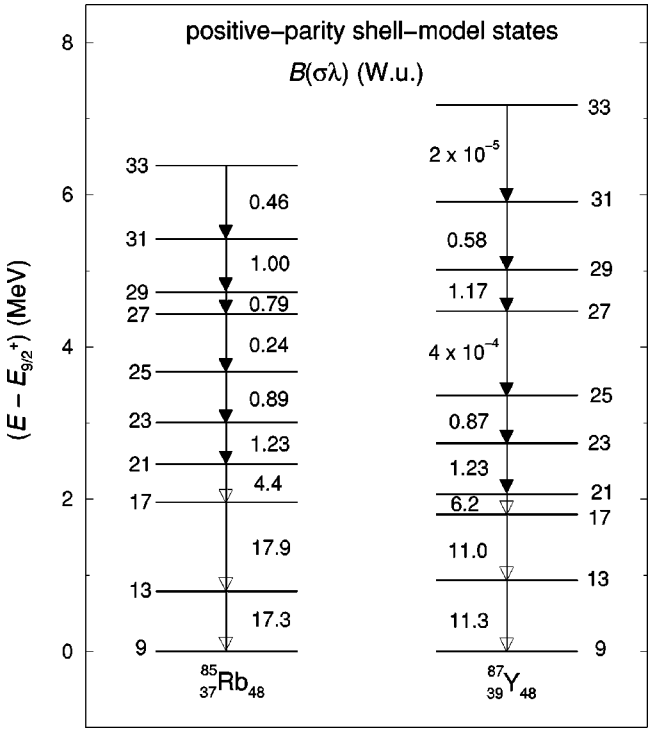

FIG. 5. Lowest-lying positive-parity shell-model states in ^{85}Rb and ^{87}Y relative to the $9/2_1^+$ state. Spins are given as $2J$. The numbers at the arrows are reduced transition strengths in W.u. $M1$ and $E2$ transitions are marked with filled and open arrow heads, respectively.

were calculated applying the surface δ interaction. These calculations have shown that 1% contributions of the configuration $\nu[(0g_{9/2})^{-2}(1d_{5/2})(0h_{11/2})]$ to the negative-parity states cause $E1$ transition strengths in the order of magnitude of the experimental ones.

An interesting phenomenon of the yrast sequence in ^{87}Y is the change of the parity at $J=27/2$ that has not been observed in the lighter $N=48$ nuclei. In the neighboring odd-mass isotone ^{85}Rb the yrast sequence includes states of positive parity up to $J=33/2$ [1–3], while states of negative parity have been found up to $J=21/2$ only. As can be seen in Fig. 4 the shell-model calculations for ^{87}Y predict the negative-parity states with $J\geqslant 29/2$ to be the yrast states which corresponds to the experimental findings.

To investigate structural differences between the isotones ^{87}Y and ^{85}Rb we have compared the results of the shell-model calculations for these nuclei. Calculated lowest-lying positive-parity states in ^{85}Rb and ^{87}Y are shown in Fig. 5. The states are graphed relative to the $9/2_1^+$ states which include mainly the configurations $\pi[(0f_{5/2}^{-2})_0 0g_{9/2}^1]\nu(0g_{9/2}^{-2})_0$ in ^{85}Rb and $\pi 0g_{9/2}^1\nu(0g_{9/2}^{-2})_0$ in ^{87}Y. These configurations predominate also in the $11/2_1^+, \ldots, 25/2_1^+$ states in the respective nucleus. The main component of the $27/2_1^+, \ldots, 33/2_1^+$ states in ^{85}Rb is $\pi[0f_{5/2}^{-1}1p_{3/2}^{-1}0g_{9/2}^1]\nu(0g_{9/2}^{-2})_8$. Thus, all states up to $J^\pi=33/2^+$ in that nucleus can be created by lifting one proton from the $(0f_{5/2},1p_{3/2})$ subshell to the $0g_{9/2}$ orbital. Compared with that, the $27/2_1^+, \ldots, 31/2_1^+$ states in ^{87}Y include two protons occupying orbitals above the subshell closure at $Z=38$ (see Table III) which may result in excitation energies higher than those of the corresponding

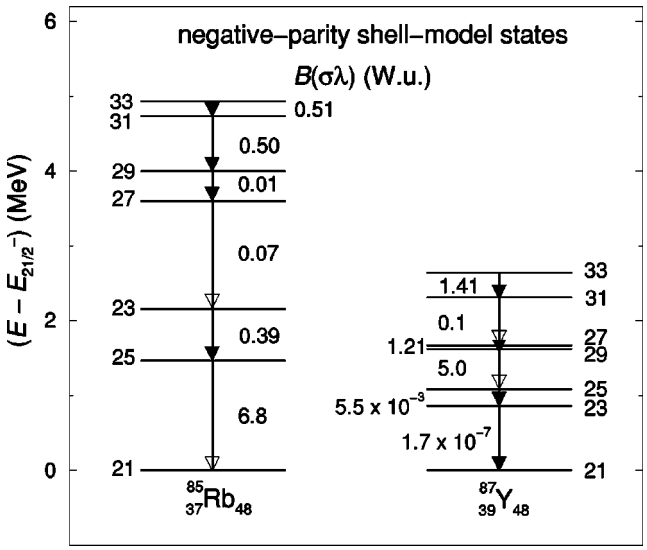

FIG. 6. Lowest-lying negative-parity shell-model states in ^{85}Rb and ^{87}Y relative to the $21/2_1^-$ state. Spins are given as $2J$. The numbers at the arrows are reduced transition strengths in W.u. $M1$ and $E2$ transitions are marked with filled and open arrow heads, respectively.

states in ^{85}Rb. Since the configuration predominating in the $27/2_1^+, \ldots, 31/2_1^+$ states in ^{87}Y is exhausted at $J=31/2$, the creation of a $33/2^+$ state requires even the change from the $\nu=5$ to a $\nu=7$ configuration (see Table III) that leads to a relatively large gap and a small $B(M1)$ value between the $31/2_1^+$ and $33/2_1^+$ states in ^{87}Y (see Fig. 5).

A comparison of lowest-lying negative-parity states in ^{85}Rb and ^{87}Y is given in Fig. 6. The states are displayed relative to the $21/2_1^-$ state that has a similar structure concerning the active nucleons in both nuclei: $\pi(0f_{5/2}^{-1})\nu(0g_{9/2}^{-2})_8$ in ^{85}Rb and $\pi[0f_{5/2}^{-1}(0g_{9/2}^2)_0]\nu(0g_{9/2}^{-2})_8$ in ^{87}Y. To generate higher spin in ^{85}Rb it is necessary to break a proton pair and lift one proton to the $1p_{1/2}$ orbital. Consequently, the $23/2_1^-$ and $25/2_1^-$ states are characterized by the configuration $\pi[0f_{5/2}^{-1}1p_{3/2}^{-1}1p_{1/2}^1]\nu(0g_{9/2}^{-2})_8$, which is exhausted at $J=25/2$. The creation of even higher spins requires therefore the excitation of two protons from the $(0f_{5/2},1p_{3/2})$ subshell into the high-j $0g_{9/2}$ orbital. The main components of the $27/2_1^-, \ldots, 33/2_1^-$ states are then of the type $\pi[(0f_{5/2}^{-2})_2 1p_{3/2}^{-1}(0g_{9/2}^2)_8]\nu(0g_{9/2}^{-2})_8$ or $\pi[0f_{5/2}^{-1}(1p_{3/2}^{-2})_0(0g_{9/2}^2)_8]\nu(0g_{9/2}^{-2})_8$. The situation in ^{87}Y is quite different. Here, the configuration of the $21/2_1^-$ state remains the main component also in the $23/2_1^-, \ldots, 33/2_1^-$ states which are generated by recoupling the spins of the involved proton orbitals (see Table III). This means that all states up to $33/2_1^-$ in ^{87}Y involve the unpaired proton in an $0g_{9/2}$ orbital and only one further proton is lifted from the $0f_{5/2}$ to the $0g_{9/2}$ orbital. This is energetically more favorable than to create $27/2_1^-, \ldots, 33/2_1^-$ states in ^{85}Rb which requires to lift two protons over the shell gap at $Z=38$ into the $0g_{9/2}$ orbital. Thus, the excitation energies of the $27/2_1^-, \ldots, 33/2_1^-$ states in ^{85}Rb are up to 2 MeV higher than those of the corresponding states in ^{87}Y as can be seen in Fig. 6.

This comparison has shown that the different location of the unpaired proton, below $Z=38$ in ^{85}Rb and above $Z=38$ in ^{87}Y, causes remarkable differences in the structure of these nuclei and, hence, in excitation energies and transition strengths. These differences may explain the experimental result that in ^{85}Rb the positive-parity states are yrast up to $J=33/2$, while in ^{87}Y the negative-parity states become energetically favored above $J=27/2$.

V. CONCLUSIONS

In the present study excited states of the $N=48$ nucleus ^{87}Y have been identified up to $J=33/2$ at $E\approx 7$ MeV with techniques of in-beam γ-ray spectroscopy. Mean lifetimes of eight levels have been deduced. Shell-model calculations performed in the model space $\pi(0f_{5/2},1p_{3/2},1p_{1/2},0g_{9/2})\nu(1p_{1/2},0g_{9/2})$ describe the majority of the observed high-spin states on the basis of $\nu=3$ and $\nu=5$ configurations. Especially the large experimental $B(M1)$ values of transitions between high-spin states with $J\geqslant 21/2$ are well reproduced. They result from a recoupling of the spins of the involved proton and neutron orbitals. A comparison of shell-model wave functions of states in ^{87}Y with those of corresponding states in the isotone ^{85}Rb explains differences between the experimentally found level structures of these nuclei.

ACKNOWLEDGMENTS

The authors would like to thank Professor W. Andrejtscheff and Dr. J. Döring for stimulating discussions. The technical assistance of W. Schulze, M. Freitag, and G. Pascovici is gratefully acknowledged.

[1] G. Winter, J. Döring, F. Dönau, and L. Funke, Z. Phys. A **334**, 415 (1989).
[2] R. Schwengner, G. Winter, J. Reif, H. Prade, L. Käubler, R. Wirowski, N. Nicolay, S. Albers, S. Eßer, P. von Brentano, and W. Andrejtscheff, Nucl. Phys. **A584**, 159 (1995).
[3] R. Schwengner, G. Winter, J. Reif, H. Prade, L. Käubler, R. Wirowski, N. Nicolay, S. Albers, S. Eßer, P. von Brentano, and W. Andrejtscheff, Phys. Scr. **T56**, 126 (1995).
[4] I. C. Oelrich, K. Krien, R. M. DelVecchio, and R. A. Naumann, Phys. Rev. C **14**, 563 (1976).
[5] C. A. Fields, F. W. N. de Boer, J. J. Kraushaar, W. W. Pratt, R. A. Ristinen, and L. E. Samuelson, Z. Phys. A **295**, 365 (1980).
[6] E. K. Warburton, J. W. Olness, C. J. Lister, J. A. Becker, and S. D. Bloom, J. Phys. G **12**, 1017 (1986).
[7] R. Wirowski, Ph.D. thesis, Universität zu Köln, 1993.
[8] M. W. Luig, S. Albers, F. Giesen, N. Nicolay, J. Rest, R. Wirowski, and P. von Brentano, Verh. Dtsch. Phys. Ges. **30**, 736 (1995).
[9] D. C. Radford, Nucl. Instrum. Methods Phys. Res. A **361**, 297 (1995).

[10] J. Theuerkauf, S. Esser, S. Krink, M. Luig, N. Nicolay, and H. Wolters, Program VS (version 6.65), Universität zu Köln, 1992.
[11] R. M. Steffen and K. Alder, in *The Electromagnetic Interaction in Nuclear Spectroscopy*, edited by W. D. Hamilton (North-Holland, Amsterdam, 1975), p. 505.
[12] K. S. Krane, R. M. Steffen, and R. M. Wheeler, Nucl. Data Tables **11**, 351 (1973).
[13] A. Krämer-Flecken, T. Morek, R. M. Lieder, W. Gast, G. Hebbinghaus, H. M. Jäger, and W. Urban, Nucl. Instrum. Methods Phys. Res. A **275**, 333 (1989).
[14] L. P. Ekström and A. Nordlund, Nucl. Instrum. Methods Phys. Res. A **313**, 421 (1992).
[15] U. Neuneyer, Program KORREL (version 3.4), Universität zu Köln, 1992.
[16] H. Morinaga and T. Yamazaki, *In-Beam Gamma-Ray Spectroscopy* (North-Holland, Amsterdam, 1976), pp. 57 and 330.
[17] G. Winter, Nucl. Instrum. Methods Phys. Res. **214**, 537 (1983).
[18] J. Lindhard, V. Nielsen, and M. Scharff, Mat. Fys. Medd. K. Dan. Vidensk. Selsk. **36** (10), 1 (1968).
[19] E. der Mateosian and A. W. Sunyar, At. Data Nucl. Data Tables **13**, 407 (1974).
[20] H. Sievers, Nucl. Data Sheets **62**, 327 (1991).
[21] P. M. Endt, At. Data Nucl. Data Tables **23**, 547 (1979).
[22] L. Funke, G. Winter, J. Döring, L. Käubler, H. Prade, R. Schwengner, E. Will, Ch. Protochhristov, W. Andrejtscheff, L. G. Kostova, P. O. Lipas, and R. Wirowski, Nucl. Phys. **A541**, 241 (1992).
[23] J. Reif, G. Winter, R. Schwengner, H. Prade, and L. Käubler, Nucl. Phys. **A587**, 449 (1995).
[24] R. Gross and A. Frenkel, Nucl. Phys. **A267**, 85 (1976).
[25] K. Ogawa, Phys. Rev. C **28**, 958 (1983).
[26] A. Amusa and R. D. Lawson, Z. Phys. A **314**, 205 (1983).
[27] K. Oxorn, S. K. Mark, J. E. Kitching, and S. S. M. Wong, Z. Phys. A **321**, 485 (1985).
[28] A. Bödeker, K. P. Lieb, C. J. Gross, M. K. Kabadiyski, D. Rudolph, M. Weiszflog, J. Eberth, H. Grawe, J. Heese, and K.-H. Maier, Phys. Rev. C **48**, 1617 (1993).
[29] D. H. Gloeckner, M. H. MacFarlane, R. D. Lawson, and F. J. D. Serduke, Phys. Lett. **40B**, 597 (1972).
[30] F. J. D. Serduke, R. D. Lawson, and D. H. Gloeckner, Nucl. Phys. **A256**, 45 (1976).
[31] M. K. Kabadiyski, F. Cristancho, C. J. Gross, A. Jungclaus, K. P. Lieb, D. Rudolph, H. Grawe, J. Heese, K.-H. Maier, J. Eberth, S. Skoda, W.-T. Chou, and E. K. Warburton, Z. Phys. A **343**, 165 (1992).
[32] G. Winter, R. Schwengner, J. Reif, H. Prade, L. Funke, R. Wirowski, N. Nicolay, A. Dewald, P. von Brentano, H. Grawe, and R. Schubart, Phys. Rev. C **48**, 1010 (1993).
[33] G. Winter, R. Schwengner, J. Reif, H. Prade, J. Döring, R. Wirowski, N. Nicolay, P. von Brentano, H. Grawe, and R. Schubart, Phys. Rev. C **49**, 2427 (1994).
[34] X. Ji and B. H. Wildenthal, Phys. Rev. C **37**, 1256 (1988).
[35] P. C. Li, W. W. Daehnick, S. K. Saha, J. D. Brown, and R. T. Kouzes, Nucl. Phys. **A469**, 393 (1987).
[36] J. Blomqvist and L. Rydström, Phys. Scr. **31**, 31 (1985).
[37] D. H. Gloeckner and F. J. D. Serduke, Nucl. Phys. **A220**, 477 (1974).
[38] D. Zwarts, Comput. Phys. Commun. **38**, 365 (1985).